

A Data Analysis Technique for the LIGO-ALLEGRO Stochastic Background Search

John T Whelan¹, Sukanta Bose², Jonathan Hanson³, Ik Siong Heng⁴, Warren W Johnson³, Martin P McHugh¹ and Peter Zhang³

¹ Department of Physics, Loyola University, New Orleans, Louisiana 70118, USA

² Washington State University, Pullman, Washington 99164, USA

³ Department of Physics and Astronomy, Louisiana State University, Baton Rouge, Louisiana 70803, USA

⁴ Department of Physics and Astronomy, University of Glasgow, Glasgow, G12 8QQ, United Kingdom

Abstract. We describe the cross-correlation measurements being carried out on data from the LIGO Livingston Observatory and the ALLEGRO resonant bar detector. The LIGO data are sampled at 16384 Hz while the ALLEGRO data are base-banded, i.e., heterodyned at 899 Hz and then sampled at 250 Hz. We handle these different sampling parameters by working in the Fourier domain, and demonstrate the approximate equivalence of this measurement to a hypothetical time-domain method in which both data streams are upsampled.

PACS numbers: 04.80.Nn, 07.05.Kf, 98.70.Vc

E-mail: jtwhelan@loyno.edu

1. Introduction

Analysis is currently underway to search for the signature of a stochastic gravitational-wave background (SGWB) by correlating the signals of the 4 km interferometer (IFO) at the LIGO Livingston Observatory (LLO)[1, 2] with the ALLEGRO resonant bar detector[3, 4, 5]. As described elsewhere[6], the LLO-ALLEGRO experiment is sensitive to a higher frequency range than the corresponding experiment using LLO and the IFOS at the LIGO Hanford Observatory (LHO)[7], thanks to the relative proximity of the ALLEGRO and LLO sites. Additionally, the ALLEGRO detector can be rotated, changing the response of the experiment to a SGWB and thus providing a means to distinguish gravitational-wave (GW) correlations from correlated noise.[8].

The results of a cross-correlation measurement using data taken during LIGO's second science run (S2) will be reported in the near future.[9] The present work describes some details of the analysis procedure used, notably the handling of the different sampling rates of the data taken by the two detectors, and the heterodyned nature of the ALLEGRO data. The procedure applied here may prove useful in coherent measurements involving data sampled at different rates, such as data from the LIGO and Virgo[10] IFOS.

2. Stochastic Gravitational-Wave Backgrounds

2.1. Definitions

A gravitational wave (GW) is described by the metric tensor perturbation $h_{ab}(\vec{r}, t)$. A given GW detector, located at position \vec{r}_{det} on the Earth, will measure a GW strain which is some projection of this tensor:

$$h(t) = h_{ab}(\vec{r}_{\text{det}}, t) d^{ab} \quad (1)$$

where d^{ab} is the detector response tensor, which is

$$d_{(\text{ifo})}^{ab} = \frac{1}{2}(\hat{x}^a \hat{x}^b - \hat{y}^a \hat{y}^b) \quad (2)$$

for an interferometer with arms parallel to the unit vectors \hat{x} and \hat{y} and

$$d_{(\text{bar})}^{ab} = \hat{u}^a \hat{u}^b \quad (3)$$

for a resonant bar with long axis parallel to the unit vector \hat{u} .

A stochastic GW background (SGWB) can arise from a superposition of uncorrelated cosmological or astrophysical sources. Such a background, if isotropic, unpolarized, stationary and Gaussian, will generate a cross-correlation between the strains measured by two detectors.[12, 13, 14] In terms of the continuous Fourier transform defined by

$$\tilde{a}(f) = \int_{-\infty}^{\infty} dt a(t) \exp(-i2\pi f[t - t_0]) , \quad (4)$$

(where t_0 is an arbitrarily-chosen time origin) the expected cross-correlation is

$$\langle \tilde{h}_1^*(f) \tilde{h}_2(f') \rangle = \frac{1}{2} \delta(f - f') P_{\text{gw}}(f) \gamma_{12}(f) \quad (5)$$

where

$$\gamma_{12}(f) = d_{1ab} d_2^{cd} \frac{5}{4\pi} \iint d^2\Omega_{\hat{n}} P^{\text{TT}\hat{n}ab}_{cd} e^{i2\pi f \hat{n} \cdot (\vec{r}_2 - \vec{r}_1)/c} \quad (6)$$

is the overlap reduction function[11] between the two detectors, defined in terms of the projector $P^{\text{TT}\hat{n}ab}_{cd}$ onto traceless symmetric tensors transverse to the unit vector \hat{n} . Figure 1 shows the overlap reduction functions for several detector pairs of interest.

$P_{\text{gw}}(f)$ is the one-sided spectrum of the SGWB. This is the one-sided power spectral density (PSD) the background would generate in an interferometer with perpendicular arms, which can be seen from (5) and the fact that the overlap reduction function of such an interferometer with itself is unity. Since the overlap reduction function of a resonant bar with itself is 4/3 (see [15] for more details), the PSD of the strain measured by a bar detector due to the SGWB would be $(4/3)P_{\text{gw}}(f)$.

A related measure of the spectrum is the dimensionless quantity Ω_{gw} , the GW energy density per unit logarithmic frequency divided by the critical energy density ρ_c need to close the universe:

$$\Omega_{\text{gw}}(f) = \frac{f}{\rho_c} \frac{d\rho_{\text{gw}}}{df} = \frac{10\pi^2}{3H_0^2} f^3 P_{\text{gw}}(f) . \quad (7)$$

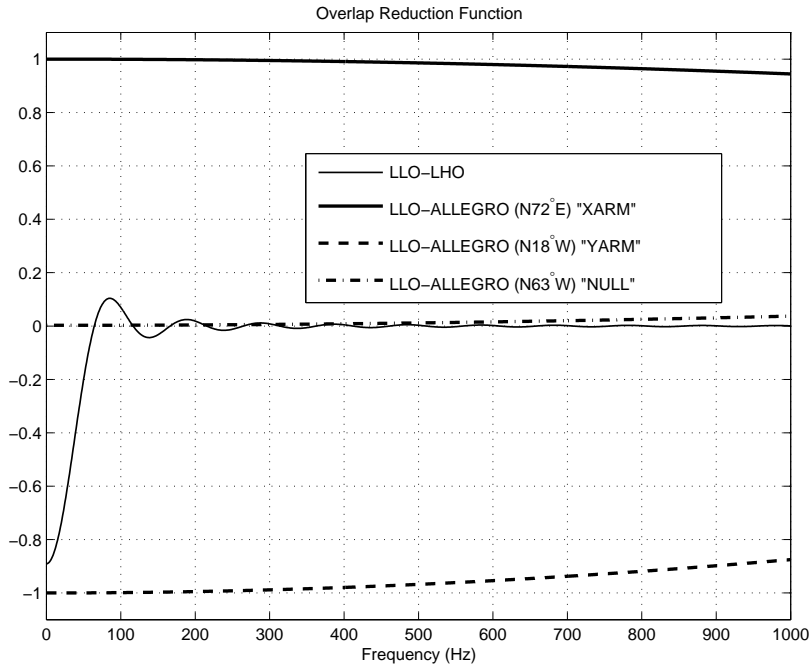


Figure 1. The overlap reduction function for LIGO Livingston Observatory (LLO) with ALLEGRO and with LIGO Hanford Observatory (LHO). The three LLO-ALLEGRO curves correspond to the three orientations in which ALLEGRO was operated during LIGO’s S2 run: “XARM” (N72°E) is nearly parallel to the x-arm of LLO (“aligned”); “YARM” (N18°W) is nearly parallel to the y-arm of LLO (“anti-aligned”); “NULL” (N63°W) is halfway in between these two orientations (a “null alignment” midway between the two LLO arms). The LLO-LHO overlap reduction function is shown for reference.

2.2. Detection Method

The standard method to search for such a background is to cross-correlate the outputs of two gravitational wave detectors [12]. If each detector signal $s_{1,2}(t)$ is assumed to be made up of a gravitational wave component $h_{1,2}(t)$ plus an instrumental noise component

$$s_{1,2}(t) = h_{1,2}(t) + n_{1,2}(t) \quad (8)$$

and the noise in the two detectors is approximately uncorrelated but significantly larger than the gravitational-wave signal, then the average cross-correlation should come from the stochastic GW background:

$$\langle \tilde{s}_1^*(f) \tilde{s}_2(f') \rangle \approx \langle \tilde{h}_1^*(f) \tilde{h}_2(f') \rangle = \frac{1}{2} \delta(f - f') P_{\text{gw}}(f) \gamma_{12}(f) \quad (9)$$

while the average auto-correlation should come from the noise:

$$\langle \tilde{s}_{1,2}^*(f) \tilde{s}_{1,2}(f') \rangle \approx \langle \tilde{n}_{1,2}^*(f) \tilde{n}_{1,2}(f') \rangle = \frac{1}{2} \delta(f - f') P_{1,2}(f) \quad (10)$$

If we construct a cross-correlation statistic

$$Y^c = \int dt_1 dt_2 s_1(t_1) Q(t_1 - t_2) s_2(t_2) = \int df \tilde{s}_1^*(f) \tilde{Q}(f) \tilde{s}_2(f) \quad (11)$$

the expected statistics of (11) are given by[16]

$$\mu_{Y^c} = \langle Y^c \rangle \approx \frac{T}{2} \int_{-\infty}^{\infty} df \gamma(|f|) P_{\text{gw}}(f) \tilde{Q}(f) \quad (12)$$

and

$$\sigma_{Y^c}^2 = \langle (Y^c - \mu_{Y^c})^2 \rangle \approx \frac{T}{4} \int_{-\infty}^{\infty} df P_1(f) P_2(f) \left| \tilde{Q}(f) \right|^2 \quad (13)$$

Using (12) and (13), the optimal choice for the filter $\tilde{Q}(f)$, given a predicted shape for the spectrum $P_{\text{gw}}(f)$ can be shown[16] to be

$$\tilde{Q}(f) \propto \frac{\gamma(|f|) P_{\text{gw}}(f)}{P_1(f) P_2(f)} \quad (14)$$

This has negligible support when $P_1(f)$ or $P_2(f)$ is large, which allows one to limit the integration in (11) to a finite range of frequencies.

In Sec. 3 we consider how the approximate continuous-time expressions (12) and (13) manifest themselves given the different discrete sampling parameters of the LIGO and ALLEGRO detectors.

3. Data Analysis Technique

3.1. Frequency-Domain Method

As described in [6], the frequency range of sensitivity correlation measurements involving the ALLEGRO resonant bar detector and the LIGO Livingston Observatory 40 km away is determined by the sensitive bandwidth of ALLEGRO [3, 5], which is limited to a band a few tens of hertz wide near 900 Hz. Due to the relatively narrow-band nature of the detector response, the data are base-banded, i.e., heterodyned at 899 Hz (during the S2 run) and downsampled to 250 Hz, so that the data represent a frequency range from $(899 - 125)$ Hz = 774 Hz to $(899 + 125)$ Hz = 1024 Hz. The LIGO data are sampled at a frequency of 16384 Hz and therefore represent frequencies ranging from -8192 Hz to 8192 Hz.

Previous work[6] proposed resampling and heterodyning the LIGO data before cross-correlation with ALLEGRO data. However, since this would involve not only downsampling by powers of two but also upsampling by a factor of 5^3 , the current approach is to approximate (11) in the frequency domain.

First, we describe the relationship between the discretely sampled data in each instrument and the underlying continuous time series $s_{1,2}(t)$. The first time series, which we will take to be the LIGO data, is sampled at a frequency $(\delta t_1)^{-1}$, which for the sake of this example we will take to be 2048 Hz.‡ Before sampling, it is low-pass filtered to avoid aliasing of higher-frequency data into the analysis band. We idealize the effects of this anti-aliasing filter by defining

$$\tilde{S}_1(f) = \begin{cases} \tilde{s}_1(f) & |f| < \frac{1}{2\delta t_1} \\ 0 & |f| > \frac{1}{2\delta t_1} \end{cases} \quad (15)$$

and writing the discretely-sampled signal as

$$S_1[j] = S_1(t_0 + j \delta t_1) \quad j = 0, \dots, N_1 - 1 \quad (16)$$

‡ The actual sampling rate is 16384 Hz, but we digitally downsample the data before analysis, a process which is straightforward enough that we don't need to explicitly address it here.

The ALLEGRO data are first heterodyned at $f_2^h = 899$ Hz to produce a continuous time series

$$s_2^h(t) = e^{-i2\pi f_2^h(t-t_0)} s_2(t) \quad (17)$$

then anti-alias filtered

$$\tilde{s}_2^h(f) = \begin{cases} \tilde{s}_2^h(f) = \tilde{s}_2(f_2^h + f) & |f| < \frac{1}{2\delta t_2} \\ 0 & |f| > \frac{1}{2\delta t_2} \end{cases} \quad (18)$$

and sampled at $(\delta t_2)^{-1} = 250$ Hz to obtain

$$S_2^h[k] = S_2^h(t_0 + k \delta t_2) \quad k = 0, \dots, N_2 - 1 \quad (19)$$

Note that this signal is now intrinsically complex. The ‘‘unheterodyned’’ time series $S_2(t) = e^{i2\pi f_2^h(t-t_0)} S_2^h(t)$ is a band-passed version of the original signal

$$\tilde{S}_2(f) = \begin{cases} \tilde{s}_2(f) & |f - f_2^h| < \frac{1}{2\delta t_2} \\ 0 & |f - f_2^h| > \frac{1}{2\delta t_2} \end{cases} \quad (20)$$

While $s_2(t)$ is real, $S_2(t)$ is not, as a result of the bandpass.

In our analysis, we construct an ensemble of statistics, each calculated by cross-correlating $T = 60$ s worth of data for each instrument, which amounts to $N_1 = T/(\delta t_1) = 122880$ points worth of LLO data and $N_2 = T/(\delta t_2) = 15000$ points worth of ALLEGRO data. The LLO data are windowed and zero-padded out to a length $M_1 = 2N_1$ and discrete Fourier transformed to produce

$$\widehat{wS}_1[\ell] = \sum_{j=0}^{N_1-1} w_1[j] S_1[j] e^{-i2\pi \ell j / M_1} = \sum_{j=0}^{N_1-1} w_1[j] S_1[j] e^{-i2\pi \ell \delta f j \delta t_1} \quad (21)$$

where $\delta f = (\delta t_1 M_1)^{-1} = (2T)^{-1} = \frac{1}{120}$ Hz for $T = 60$ s, and $\ell = -N_1, \dots, N_1 - 1$. Meanwhile, the ALLEGRO data are windowed and zero-padded out to a length $M_2 = 2N_2$ and discrete Fourier transformed to produce

$$\begin{aligned} \widehat{wS}_2[\ell] &= \sum_{k=0}^{N_2-1} w_2[k] S_2^h[k] e^{-i2\pi \ell k / M_2} e^{i2\pi f_2^h k \delta t_2} \\ &= \sum_{k=0}^{N_2-1} w_2[k] S_2^h[k] e^{-i2\pi (\ell \delta f - f_2^h) k \delta t_2} \end{aligned} \quad (22)$$

where $\delta f = (\delta t_2 M_2)^{-1}$ is the same frequency resolution as before, and $\ell = \frac{f_2^h}{\delta f} - N_2, \dots, \frac{f_2^h}{\delta f} + N_2 - 1$. With these definitions,

$$\delta t_{1,2} \widehat{wS}_{1,2}[\ell] \sim \tilde{S}_{1,2}(\ell \delta f) \quad (23)$$

so if we construct a frequency-domain optimal filter $\tilde{Q}(f)$, we can obtain an approximate analogue $Y \sim Y^c$ for the Y^c defined in (11) by constructing the statistic

$$Y = \sum_{\ell=\ell_{\min}}^{\ell_{\max}} \delta f (\delta t_1 \widehat{wS}_1[\ell])^* \tilde{Q}(\ell \delta f) (\delta t_2 \widehat{wS}_2[\ell]) \quad (24)$$

where $(\ell_{\min} \delta f, \ell_{\max} \delta f)$ is the frequency range over which $\tilde{Q}(f)$ has significant support. Because of the factor of $P_1(f)P_2(f)$ in the denominator of (14), this is limited to a subset of the frequency ranges associated with both the LLO and ALLEGRO data, as illustrated in Figure 2.

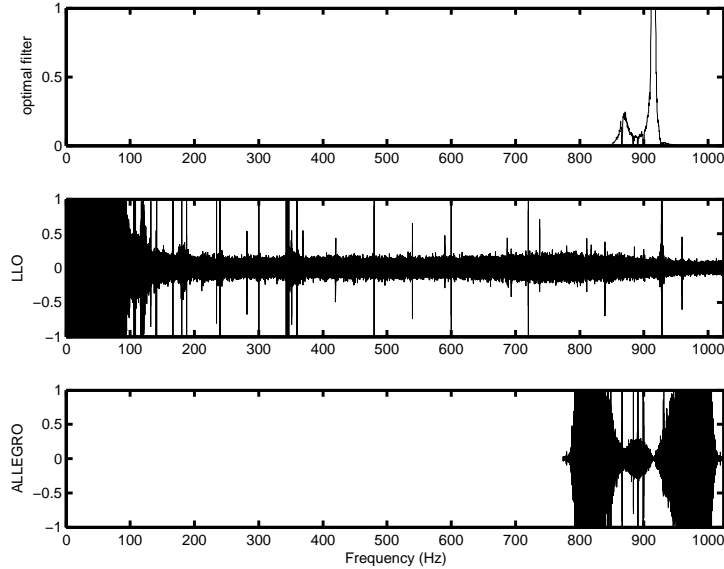


Figure 2. The frequency ranges covered by Fourier-transformed LLO and ALLEGRO data and the optimal filter used for analysis. The vertical scales are arbitrary and the data are meant to be illustrative only. If LLO data are downsampled to 2048 Hz, their discrete Fourier transform covers frequencies from -1024 Hz to 1024 Hz. The ALLEGRO data are heterodyned at 899 Hz and sampled at 250 Hz, which makes the frequencies represented range from 774 Hz to 1024 Hz. The optimal filter has non-negligible support only for $850 \text{ Hz} \lesssim f \lesssim 950 \text{ Hz}$, so those are the only frequencies included in the cross-correlation.

3.2. Time-Domain Equivalent

In this section we consider a time-domain cross-correlation equivalent to the discrete frequency-domain approximation (24) and explicitly calculate the discrete-time equivalents of (12) and (13).

One conceptually simple approach to cross-correlating these two data streams in the time domain would be to upsample both to the same sampling frequency. This should work as long as the ratio of the sampling rates is a rational number. We define r_1 and r_2 as the smallest integers such that

$$\frac{\delta t_1}{\delta t_2} = \frac{r_1}{r_2} \quad (25)$$

(in the present example, $r_1 = 125$ and $r_2 = 1024$) and then define

$$\delta t = \frac{\delta t_1}{r_1} = \frac{\delta t_2}{r_2} \quad (26)$$

(In the present example, $(\delta t)^{-1} = 256000$ Hz.) These upsampled time series would then each contain

$$N = N_1 r_1 = N_2 r_2 \quad (27)$$

points. (In the present example, $N = 15360000$.) The method used to upsample the data does not interest us, since we won't actually perform the time-domain

upsampling. Instead, we idealize the result as the discrete sampling of the band-passed time series $S_1(t)$ and $S_2^h(t)$:

$$S_1^r[J] = S_1(t_0 + j \delta t) \quad J = 0, \dots, N \quad (28)$$

$$S_2^{hr}[K] = S_2^h(t_0 + K \delta t) \quad K = 0, \dots, N \quad (29)$$

If we also assume that $f_2^h + 1/2\delta t_2 < 1/2\delta t$, there is no loss of information in going between the heterodyned and non-heterodyned data streams at the higher sampling rate. It is thus reasonable to think of the cross-correlation statistic as

$$\begin{aligned} Y^r &= \sum_{J=0}^{N-1} \delta t \sum_{K=0}^{N-1} \delta t w_1^r[J] S_1^r[J]^* Q^r[J-K] w_2^r[K] S_2^r[K] \quad (30) \\ &= \sum_{J=0}^{N-1} \delta t \sum_{K=0}^{N-1} \delta t w_1^r[J] S_1^r[J]^* Q^r[J-K] e^{i2\pi f_2^h K \delta t} w_2^r[K] S_2^{hr}[K] \end{aligned}$$

(The factors of δt are to facilitate comparison with the continuous-time idealization.) The optimal filter $Q[J-K]$ depends only on the difference between the two indices, consistent with the assumption that we're considering *stationary* random processes, but the introduction of the two N -point window functions[§] $w_{1,2}[J]$ (assumed to be real) allows us to control edge effects by smoothing out the onset and ending of the analyzed data, and the complex exponential accounts for the heterodyning.

On the other hand, the analysis is not actually done with the upsampled time series $S_1^r[J]$ and $S_2^{hr}[K]$, but with the original $S_1[j]$ and $S_2^h[k]$. So if we calculated a time-domain cross-correlation statistic, it would be

$$Y = \sum_{j=0}^{N_1-1} \delta t_1 \sum_{k=0}^{N_2-1} \delta t_2 w_1[j] S_1[j]^* Q^h[j,k] w_2[k] S_2^h[k] \quad (31)$$

Again, the bandpass tells us that the upsampled data streams don't have any higher-frequency content that's not present in the original ones. So we should get roughly the same cross-correlation statistic if we limit the sum in (30) to J an integer multiple of r_1 and K an integer multiple of r_2 , and then multiply by $r_1 r_2$ to compensate for having taken fewer terms. This means $Y^r \approx Y$ with

$$Q^h[j,k] = Q^r[r_1 j - r_2 k] e^{i2\pi f_2^h k \delta t_2} \quad (32)$$

Since the sums over j and k in (31) both range from 0 to $N-1$, the argument of $Q[j-k]$ ranges from $-(N-1)$ to $N-1$, so a discrete Fourier transform (DFT) of Q will need to include at least $2N-1$ points. Since it is often more convenient to work with a $2N$ -point DFT than a $2N-1$ -point one (e.g., if N is a power of two or a product of small primes), we will in general zero-pad $Q[m]$ out to $M \geq 2N-1$ points, with the "extra" values (i.e., those with $N-1 < m \leq M-1$) defined by

$$Q[m] = \begin{cases} 0 & N-1 < m < M-(N-1) \\ Q[m-M] & M-(N-1) \leq m < M \end{cases}, \quad (33)$$

before defining the discrete Fourier transform

$$\hat{Q}[\ell] = \sum_{m=0}^{M-1} e^{-i2\pi m \ell / M} Q^r[m] = \sum_{m=-(N-1)}^{N-1} e^{-i2\pi m \ell / M} Q^r[m]. \quad (34)$$

[§] The analysis of windowing effects described here is a generalization of that described in [17] and used in [7] for two data streams sampled at the same rate.

We can transform (31) into the frequency domain using the inverses of (4) and (34):

$$S_{1,2}(t) = \int_{-\infty}^{\infty} df e^{i2\pi f(t-t_0)} \tilde{S}_{1,2}(f) \quad (35)$$

$$Q^r[m] = \frac{1}{M} \sum_{\ell=0}^{M-1} e^{i2\pi m\ell/M} \hat{Q}[\ell] \quad (36)$$

the result is

$$Y = \frac{1}{M} \sum_{\ell=0}^{M-1} (\delta t)^2 \hat{Q}[\ell] \left(\int_{-\infty}^{\infty} df_1 \widehat{W}_1([f_\ell - f_1]T) \tilde{S}_1(f_1) \right)^* \times \left(\int_{-\infty}^{\infty} df_2 \widehat{W}_2([f_\ell - f_2]T) \tilde{S}_2(f_2) \right) \quad (37)$$

where $\delta f = (M \delta t)^{-1}$, $f_\ell = \ell \delta f$, and the transformed window

$$\widehat{W}_{1,2}(x) = \sum_{j=0}^{N-1} e^{-i2\pi x j/N_{1,2}} w_{1,2}[j] \quad (38)$$

is equivalent to an N_1 or N_2 -point discrete Fourier transform, but not limited to integer arguments. Note that by construction $\widehat{W}_{1,2}(x)$ is periodic with period $N_{1,2}$: $\widehat{W}_{1,2}(x + N_{1,2}) = \widehat{W}_{1,2}(x)$.

3.3. Mean and Variance of the Statistic

We can get expressions for the expected mean and variance of (37) by applying (9) and (10), and noting that if we define $c_{ij}(f)$ by

$$\langle \tilde{s}_i(f) \tilde{s}_j(f') \rangle = \delta(f - f') c_{ij}(f) \quad (39)$$

so that $c_{ii}(f) = \frac{1}{2} P_i(f)$ and $c_{12}(f) = \frac{1}{2} P_{\text{gw}}(f) \gamma_{12}(f)$, then

$$\langle \tilde{S}_i(f) \tilde{S}_j(f') \rangle = \delta(f - f') C_{ij}(f) \quad (40)$$

where

$$C_{ij}(f) = \begin{cases} c_{ij}(f) & f_2^h - \frac{1}{2\delta t_2} < f < \min\left(\frac{1}{2\delta t_1}, f_2^h + \frac{1}{2\delta t_2}\right) \\ 0 & \text{otherwise} \end{cases} \quad (41)$$

The mean is

$$\mu = \langle Y \rangle = \frac{1}{M} \sum_{\ell=0}^{M-1} (\delta t_1)(\delta t_2) \hat{Q}[\ell] \times \int_{-\infty}^{\infty} df \widehat{W}_1([f_\ell - f]T)^* \widehat{W}_2([f_\ell - f]T) C_{12}(f) \quad (42)$$

As before, the restricted support of $C_{12}(f)$ means that we can change the limits of the frequency integral from $(-\infty, \infty)$ to $(-\frac{1}{2\delta t}, \frac{1}{2\delta t})$.

In this case, the periodicity of the windowing functions means that if they're sufficiently sharply peaked about zero argument, we must have $(f_\ell - f)T$ approximately equal to $0 \bmod N_1$ and $0 \bmod N_2$. But since N is the lowest common multiple of N_1 and N_2 , this is equivalent to the condition that $(f_\ell - f)T \approx 0 \bmod N$, which is true for at most one frequency in the range $f_2^h - \frac{1}{2\delta t_2} < f < \min\left(\frac{1}{2\delta t_1}, f_2^h + \frac{1}{2\delta t_2}\right)$, and that

frequency is always the positive f_ℓ . The windowing thus allows us to replace $C_{12}(f)$ with $C_{12}(f_\ell)$ in (42) and obtain

$$\begin{aligned} \mu &\approx \frac{1}{M} \sum_{\ell=\ell_{\min}}^{\ell_{\max}} (\delta t_1)(\delta t_2) \widehat{Q}[\ell] c_{12}(f_\ell) \\ &\quad \times \int_{-1/(2\delta t)}^{1/(2\delta t)} df \widehat{W}_1([f_\ell - f]T)^* \widehat{W}_2([f_\ell - f]T) \end{aligned} \quad (43)$$

where the limits on the sum over ℓ are those such that

$$f_2^h - \frac{1}{2\delta t_2} < f_\ell < \min\left(\frac{1}{2\delta t_1}, f_2^h + \frac{1}{2\delta t_2}\right) \quad (44)$$

The integral can be evaluated [using (38)] as

$$\begin{aligned} &\int_{-1/(2\delta t)}^{1/(2\delta t)} df \widehat{W}_1([f_\ell - f]T)^* \widehat{W}_2([f_\ell - f]T) \\ &= \sum_{j=0}^{N_1-1} \sum_{k=0}^{N_2-1} w_1[j] w_2[k] \int_{-1/(2\delta t)}^{1/(2\delta t)} df e^{i2\pi(f_\ell - f)(jr_1 - kr_2)\delta t} \\ &= \frac{1}{\delta t} \sum_{j=0}^{N_1-1} \sum_{k=0}^{N_2-1} \delta_{jr_1, kr_2} w_1[j] w_2[k] = \frac{1}{\delta t} \frac{N}{r_1 r_2} \overline{w_1 w_2} \end{aligned} \quad (45)$$

Note that the average of the product of the windows is taken only over the points for which both windows ‘‘coexist’’ given their different sampling rates:

$$\overline{w_1 w_2} = \frac{r_1 r_2}{N} \sum_{n=0}^{N/(r_1 r_2)-1} w_1[nr_2] w_2[nr_1] \quad (46)$$

This then tells us

$$\mu \approx \overline{w_1 w_2} \frac{T}{2} \sum_{\ell=\ell_{\min}}^{\ell_{\max}} \delta f (\delta t \widehat{Q}[\ell]) \gamma(f_\ell) P_{\text{gw}}(f_\ell) \quad (47)$$

where we have used again the definition $\delta f = 1/(M \delta t)$.

As before, we can identify (47) (up to the factor of $\overline{w_1 w_2}$) as a discrete approximation to the usual continuous-time expression if we note that (34) relates the discrete and continuous Fourier transforms according to $\delta t \widehat{Q}[\ell] \sim \widetilde{Q}(f_\ell)$.

Note that if we design the filter in the frequency domain and chose $\widehat{Q}[\ell]$ to be real, (47) tells us that the mean value of the statistic is real as long as any underlying correlation between the two data streams is time-symmetric. However, the band-passing means that $s_2(t)$ is complex, and therefore the statistic Y is as well.

Since Y is complex, we consider the variance of $x := \text{Re} Y = \frac{Y+Y^*}{2}$ and $y := \text{Im} Y = \frac{Y-Y^*}{2}$ separately. This ultimately comes down to calculating $\langle Y^2 \rangle$ and $\langle YY^* \rangle$, and specifically the contribution from the auto-correlations.

In fact, the dominant contribution to $\langle Y^2 \rangle$ vanishes because it contains $\langle \widetilde{S}_2(f') \widetilde{S}_2(f) \rangle$. Now, this is zero unless both f and f' lie in the range $[f_2^h - \frac{1}{2\delta t_2}, f_2^h + \frac{1}{2\delta t_2}]$, which in particular means both f and f' are positive. If it lies in that range, it is equal to

$$\langle \widetilde{s}_2(f') \widetilde{s}_2(f) \rangle = \langle \widetilde{s}_2(-f')^* \widetilde{s}_2(f) \rangle = \delta(f + f') \frac{P_2(|f|)}{2} \quad (48)$$

but this vanishes unless f and f' have the opposite sign. Thus there is no combination of frequencies for which $\langle \tilde{S}_2(f') \tilde{S}_2(f) \rangle$ is non-zero.

This then means that the real and imaginary parts of Y both have a variance of

$$\sigma_x^2 \approx \sigma_y^2 = \frac{1}{2} \langle Y^* Y \rangle \approx \frac{T}{8} \frac{1}{w_1^2 w_2^2} \sum_{\ell=0}^{M-1} \delta f \left| (\delta t \hat{Q}[\ell]) \right|^2 P_1(|f_\ell|) P_2(|f_\ell|) \quad (49)$$

where again the window average is conducted over the $N/(r_1 r_2)$ points where the windows “line up”.

4. Conclusions

We have described the data analysis method used for cross-correlating in the frequency domain two data streams sampled at different rates, one of which is also heterodyned prior to digitization. We have illustrated heuristically how this approximates a continuous-time description, and also its equivalence to a hypothetical cross-correlation in the time domain using upsampled data streams. This frequency-domain technique allows us to efficiently cross-correlate data from different detectors with different sampling parameters, and is being applied to LIGO and ALLEGRO data taken during LIGO’s second science run.

Acknowledgments

We would like to thank everyone at the LIGO and ALLEGRO projects and especially the LSC’s stochastic analysis group. JTW gratefully acknowledges the University of Texas at Brownsville and the Albert Einstein Institute in Golm. ISH gratefully acknowledges Louisiana State University and Albert Einstein Institute in Hannover. Additional thanks to Lucio Baggio. This work was supported by the National Science Foundation under grants PHY-0140369 (Loyola), PHY-0300609 (Loyola), PHY-0355372 (Loyola), PHY-0239735 (WSU), and PHY-9970742 (LSU) and by the Max-Planck-Society.

References

- [1] <http://www.ligo-la.caltech.edu/>
- [2] Abbot B et al (LIGO Scientific Collaboration) 2004 *Nucl. Instrum. Methods* **A517** 154
- [3] <http://gravity.phys.lsu.edu/>
- [4] Mauceli E et al 1996 *Phys. Rev.* **D54** 1264
- [5] Harry G M 1999, thesis, University of Maryland
- [6] Whelan J T et al 2003 *Class. Quantum Grav.* **20** S689
- [7] Abbot B et al (LIGO Scientific Collaboration) 2004 *Phys. Rev.* **D69** 122004
- [8] Finn L S and Lazzarini A *Phys. Rev.* **D64** 082002
- [9] Abbot B et al (LIGO Scientific Collaboration) 2005 (in preparation)
- [10] <http://www.virgo.infn.it/>
- [11] Flanagan É É 1993 *Phys. Rev.* **D48** 2389
- [12] Christensen N 1992 *Phys. Rev.* **D46** 5250
- [13] Allen B 1997 in *Proceedings of the Les Houches School on Astrophysical Sources of Gravitational Waves*, eds Marck J A and Lasota J P, Cambridge, 373
- [14] Maggiore M 2000 *Phys. Rep.* **331** 28
- [15] J. T. Whelan, “Stochastic Gravitational Wave Measurements with Bar Detectors: Dependence of Response on Detector Orientation,” in process.
- [16] Allen B and Romano J D 1999 *Phys. Rev.* **D59** 102001
- [17] Whelan J T 2004 LIGO technical document LIGO-T040125-00-Z; <http://www.ligo.caltech.edu/docs/T/T040125-00.pdf>